PCCP

Accepted Manuscript

ROYAL SOCIETY OF CHEMISTRY

www.rsc.org/pccp

Gas phase dynamics of triplet formation in benzophenone

Gloria Spighi, Marc-André Gaveau, Jean-Michel Mestdagh, Lionel Poisson and Benoît Soep*

Laboratoire Francis Perrin, CNRS URA 2453, CEA, IRAMIS, Lidyl, Bat 522
F-91191 Gif/Yvette, France

Abstract

Benzophenone is a prototype molecule for photochemistry in the triplet state through its high triplet yield and reactivity. We have investigated its dynamics of triplet formation in the isolated gas phase conditions via femtosecond and nanosecond time resolved photoelectron spectroscopy. This represents the complete evolution from the excitation in S_2 to the final decay of T_1 to the ground state S_0. We have found that the triplet formation can be described almost as a direct process in preparing T_1, the lowest reacting triplet state, from the S_1 state after $S_2 \rightarrow S_1$ internal conversion. The molecule was also deposited by a pick-up technique on cold argon clusters providing a soft relaxation medium without evaporation of the molecule and the mechanism was identical. This cluster technique is a model for medium influenced electronic relaxation and provides a continuous transition from the isolated gas phase to the relaxation dynamics in solution.

Submitted to PCCP

*Corresponding author: benoit.soep@cea.fr

Introduction

Most of the photochemistry in organic molecules proceeds through long lived states such as triplet states[1]. There, they have been electronically activated as open shell molecules and they can encounter barrierless reactions through collisions during their long lifetime. Benzophenone (diphenyl ketone, scheme 1) represents a paradigmatic example for the photochemistry of simple

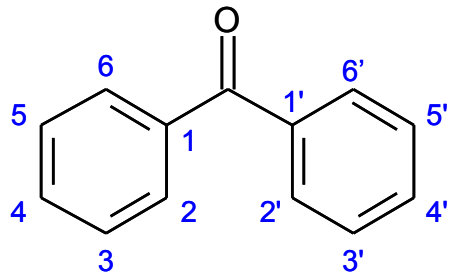

Scheme 1

organic molecules, owing to its triplet yield close to unity and thus to the variety of reactions in which it is involved. A typical reaction is the hydrogen abstraction reaction via its activated oxygen atom. As a general property, triplet states of organic molecules are reactive through their biradical character[2]. Indeed the two unpaired electrons avoid Pauli repulsion and occupy well separated spatial regions in the given molecule. Since the electron in the π* orbital is delocalized on the phenyl rings, as shown by the greater planarity of the ππ* and nπ*states compared to the fundamental[3], triplet benzophenone can be described with one unpaired electron located on oxygen, while the other is over the two phenyl rings. In the diradical triplet state, the electron-deficient oxygen n-orbital is electrophilic and therefore interacts with weak C-H bonds, resulting in hydrogen abstraction to complete the half-filled n-orbital.

In photochemistry, metastable triplet states with too low oscillator strength are prepared by singlet excitation and subsequent intersystem crossing (ISC). Efficient intersystem crossing in organic molecules is a puzzling issue since spin-orbit coupling V_{SO} is rather small for light atoms resulting in small rate constants k_{ISC} for intersystem crossing. If one thinks in terms of the Fermi golden rule description[4] of ISC, the crossing rate is $k_{ISC} \propto (V_{SO})^2$. This issue has recently been challenged for benzene, close to the opening of the so-called "channel 3" to isomerization [5, 6] There, spin-orbit coupling is dramatically increased by vibronic effects in the vicinity of the conical intersection to prefulvene. This results in a very fast buildup of T states in benzene, in the

femtosecond range comparable to internal conversion. Another example is found in copper metalloporphyrin systems where the copper atom links the S ($^1\pi\pi^*$) and T ($^3\pi\pi^*$) states on the porphyrin ring [7], but there, this is an indirect spin-orbit coupling through a charge transfer state. In contrast, there seems to exist for benzophenone, a direct strong coupling between equilibrated $S_1(^1n\pi^*)$ and the isoenergetic T_2 ($^3\pi\pi^*$) that results in rapid picosecond, triplet formation as observed in the condensed phase [8, 9].

Benzophenone is non planar in its ground state due to the steric repulsion of the H_2 and $H_{2'}$ atoms on the phenyl rings. The two rings are twisted with an angle of 38° and an overall C_2 geometry [3]. The first excited singlet state of low absorption at 26244 cm^{-1} [10, 11], is of $n\pi^*$ configuration, while the intense $\pi\pi^*$ excitation has maxima at 35500 and 40300 cm^{-1} in cyclohexane. The equilibrium geometry of electronically excited benzophenone is more planar owing to the delocalization of the π^* orbital over the whole molecule[3]. This appears clearly in the excitation spectrum of S_1, through an extended vibrational progression of the ring symmetric torsional mode [10,11]. The lowest triplet, $T(n\pi^*)$, is expected at 24044 cm^{-1} in the gas phase, from the 2200 cm^{-1} S-T splitting in cryogenic crystals [12]. The second lowest triplet state is believed to be of $\pi\pi^*$ nature and is calculated at 26316 cm^{-1} [13], in quasi-resonance with S_1. This resonance should drive a non negligible spin-orbit coupling matrix element between $S_1(n\pi^*)$ and T_2 ($\pi\pi^*$) along El Sayed rules [14, 15]. The basis of this rule is the coupling of the n in-plane lone pair orbital, with the out-of-plane π^* orbital by the spin-orbit operator. This has been considered as the cause of the very low fluorescence yield of benzophenone due to a picosecond, surprisingly fast intersystem crossing (ISC) [8, 9]. Also, this should have been at the origin of the long lived emission of benzophenone excited at 347 nm[16], through the excitation of levels with strongly mixed singlet and triplet character. However, the other main consequence of strong S-T mixing, the ultrafast ISC competing with other electronic relaxation processes, has not been investigated in the gas phase for benzophenone as in the case of benzene[6], this was the lead for our observations.

Rapid, picosecond ISC has been observed in solutions for benzophenone [8,9]. Recently [17], the time evolution from the S_2 state has also been detected in the condensed phase and it was shown that an ultrafast decay to the S_1 state (0.53 ps) precedes fast intersystem crossing. There are some indications of a transient triplet level accessed from S_1 [9]. Intersystem crossing to T_1 is a really specific mechanism for its efficiency in benzophenone as compared to other organic molecules.

Its rate is faster by 10^3 times as compared to similar aromatic cetones, such as fluorenone with a slow ISC to T_1 [18]. Since the characterization of the intersystem crossing mechanism is crucial for the photochemistry of benzophenone, we have revisited here the time evolution in the gas phase of cooled benzophenone after excitation to the second singlet S_2 at 266 nm. At the same time, we have investigated also benzophenone deposited on argon clusters in the same experimental conditions. This evolution has been monitored from femtoseconds up to early microseconds. The idea of such experiments is to bridge the gap between gas phase and condensed phase experiments, since benzophenone is located and solvated at the surface of an argon cluster. There, the time evolution observed in both cases shows a sequential process involving a S_2-S_1 ultrafast relaxation followed by a fast intersystem crossing and subsequent decay. Indeed the observed kinetics do not match a parallel mechanism where intersystem crossing would occur during the S_2-S_1 internal conversion, owing to the abovementioned enhanced couplings, but it is perfectly fit by a sequential $S_2 \rightarrow S_1 \rightarrow T \rightarrow S_0$ evolution.

Experimental

Two types of experiments have been conducted on supersonically cooled gas phase benzophenone excited at 266 nm in S_2: femtosecond and submicrosecond time resolved spectroscopy using pump/probe methods and electron or ion detection.

The femtosecond time resolved setup has been described in details in reference[19], cluster deposition effects in [20] and the nanosecond system in [21]. In the femtosecond experiments, a free jet of benzophenone has been produced by entrainment of benzophenone vapor at room temperature in a supersonic jet of helium. Benzophenone is placed in a small chamber posterior to a pulsed valve (General Valve). Deposition on argon clusters was obtained by passing a beam of clusters over a heated oven containing benzophenone at ~100°C. After passing a 1 mm skimmer, the jet entered the main chamber, equipped with a time-of-flight mass spectrometer (TOF-MS) and a velocity map imaging (VMI) spectrometer. The latter allows monitoring of either the ions or the electrons produced upon photoionization (pump/probe experiment). For each pump/probe delay, the raw images of the photoelectrons were accumulated over several hundred laser shots. To obtain the electron kinetic energy distribution, the raw images were transformed by the pBASEX-algorithm[22], which yields the photoelectron spectrum as a function of the delay and allows separating the polarised and unpolarised parts of the image.

A 20 Hz femtosecond Ti:Sa oscillator/amplifier laser system was used, which has been described previously[19]. The third harmonic (10-50 μJ) of the Ti:Sapphire is at 265 nm and due to the bandwidth of a fs-pulse we will refer to this wavelength as '266 nm', thus comprising the ns 4th harmonic of the YAG laser. The excited state population was then probed with either the fundamental of the Ti:Sapphire (between 796 nm and 800 nm, 100-700 μJ) or the second harmonic around 398 nm (50-100 μJ) in a 'low' multiphoton process. The intensities of the pump or probe beams were attenuated until one-colour signals were minimized to <5% of the maximum signal. The pump beam was focused about 14 cm away from the interaction region, and the focus of the probe beam lays 5 cm away..This yielded intensities ≈10^{12} W/cm^{2}. In time delay scans, the probe beam was delayed with respect to the pump via a delay line that was actuated by a computer-controlled stepper motor. The intervals between two data points were adjusted to the decay signal and are not equidistant. Before the rise of the signal and at longer delays the time intervals were larger (between 100 and 500 fs) than around time zero where data points were taken about every 8 fs. Both beams were polarised horizontally within these experiments and overlapped in a small angle setup in the interaction region. The cross-correlation was found to be around 100 fs. Additional experiments were carried out with the polarization of the pump and probe beam perpendicular to each other. All time resolved traces were averaged for two to six scans.

The nanosecond/submicrosecond pump probe experiment was performed by expansion of a helium benzophenone mixture obtained by passing helium over warm benzophenone. Benzophenone was excited in S_2 in the quasi-continuous part of the spectrum with the 4th harmonic of a Nd:YAG laser at 266 nm. An ArF (193 nm) excimer laser was triggered with a variable ns-μs electronic delay between -200 ns and 1μs. The laser beams were collinear but counter propagating and were unfocussed. The excimer beam (0.5mJ) was collimated to the 2mm size of the 266 nm beam (≈0.1mJ). VMI was also applied to the photoelectron detection and analysed the same way. The μs limit in time detection is determined by the decay of the overlap of the probe with the moving excited set of benzophenone molecules within the supersonic beam moving at 1800 m/s.

Results

The time evolution of benzophenone excited in S_2 has been observed by time resolved photoelectron spectroscopy from early femtoseconds to microseconds. The purpose is to disentangle the competition between the various decays S_2-S_1 internal conversion, S_2-T_n intersystem crossing, S_1-$T_{2,1}$ intersystem crossing, occurring on different timescales. The seminal case for these studies is that of ISC in pyrazine by Suzuki et al.[23].

The evolution in the femtosecond time range has been monitored by 266 nm pump (exciting the origin band in S_2) and either 400 or 800 nm probes, which generate signals revealing different aspects of the evolution. With the 800 nm probe the signal was sufficiently intense to allow probing the molecule deposited on argon clusters. Optical time delays up to 300 ps have been used and for longer times, a nanosecond 266 nm excitation with a 10 ns-1000 ns delayed, one photon ionisation 193 nm probe has been applied. Thus, the evolution of the system has been continuously monitored over 5 decades of time.

Femtosecond probing with 400nm

The angular distribution of the photoelectron spectrum is polarised along the light polarisation and can be represented along the classical expansion in even order Legendre polynomials. The photoelectron spectrum is polarised mostly with a second order component, β_2=0.3±0.1 in the expansion commonly used for multiphoton excitation and derived from the one photon expression with β_2 [24] :

$$I(\theta,t) = \sigma(t)\,[1 + \beta_2(t) P_2(\cos\theta) + \beta_4(t) P_4(\cos\theta) + \beta_6(t) P_6(\cos\theta) + \ldots] \quad (1)$$

The expansion in P_0 and P_2 Legendre components has been performed with the pBasex method [22], implemented under LabView. The resulting spectra reveal broad bands with coarse structure, up to 1.7 eV. The photoelectron spectra are analysed as in figure 1, by a fit with a sum of Gaussian components. These bands evolve in intensity after the autocorrelation of the pump and probe lasers without any noticeable energy shift. Here, in figures 1 and 2, the intensities I(E) have been multiplied by the abscissa E as I(E)×E to visualise better the bands close to the origin. The P_2 expansion of the photoelectron spectrum is very similar to the P_0 expansion but with narrower bands. As we shall describe, we do not extract the same information from the same bands in the P_0 and P_2, indicating different contributions at the same electron energy.

Examining the time evolution of the signals corresponding to these bands as in figure 2, for all bands with electron energy > 0.2 eV, an initial rapid decay appears with a 150±30 fs time constant and further evolution. On the other hand, this 400 nm probe is especially helpful in revealing information at short times (t<1ps). Some evolution aspects, like the clear oscillations, will be considered later in the paper. The band labelled 1 (0.1 eV) and traced in black, reveals an initial rise instead of a decay, but with the same 150 fs time constant. For the other bands (2, 3), the decay is biexponential with the initial constant τ_1=150 fs (identical to the rise observed for band 1), followed by a decay with τ_2=5±0.5 ps. The initial rise observing band 1 is only seen in the P_0 component not on the P_2 one. This results from the stronger polarisation of the electrons from the resonantly ionised from S_2 as compared to those from relaxed the S_1 or T_1 states.

All bands, on the other hand, show a triple exponential evolution with the 150 fs initial rise or decay followed by a 5 ps decay into a plateau further evolving beyond a ns timescale. The ratios of the short 150 fs component (τ_1), medium 5 ps (τ_2) and long ns (τ_3) components are functions of the photoelectron energy, as seen for example in figures 2 and 1. Band 1 at 0.1 eV has the highest medium time component and band 3, the lowest medium component. Thus, each band: 0, 1, 2 informs more specifically on a time component, i.e an element of the states traversed by the evolving wavepacket.

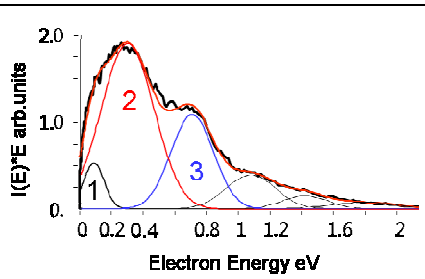

Fig 1: Isotropic component P_0 of the photoelectron spectrum in the 266/400 nm pump/probe experiment. The signal, given as I(E)×E and summed over the time evolution, is simulated with a sum of Gaussian functions centred at 0.1 eV(1,black), 0.3 eV (2, red), 0.7 eV (3, blue) and others of higher energy.

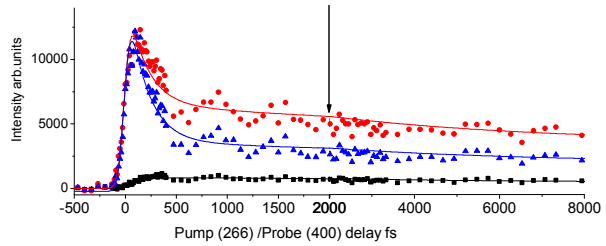

Fig 2: Time evolution of the photoelectron bands at 0.1, 0.3 and 0.7 eV selected in figure 1 and displayed with the same colour code. Note the change of the horizontal linear scale at the arrow: [-500, 2000 fs] on the left, [2000, 800 fs] on the right..

Also, the time evolution in the 0-3000 fs domain, shows oscillations with a period of 550±20 fs. These oscillations have in common the phase for all electron energies, whether the signal initially increases or decreases. In the simulation of figure 3 (band 2 in figure 1) with the oscillation period of a $\sin(2\pi.t/T- \phi)$ function (T=550fs), a biexponential decay (τ_1=150 fs / τ_2=5000 fs), the first maximum for the oscillations is obtained at ~300fs, relative to the autocorrelation time. The oscillations damp in 2 ps. The simulations are obtained by a least square fit on the time constants.

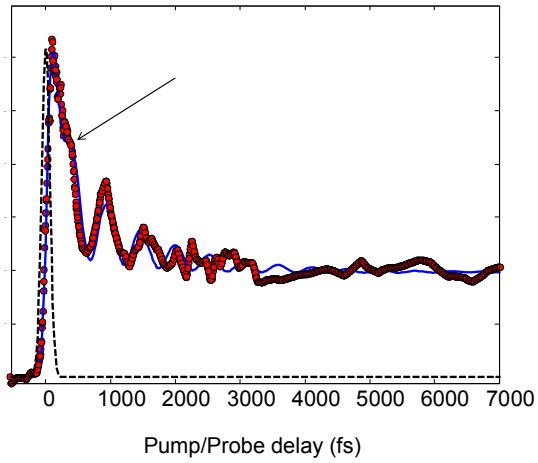

Fig 3 : Data (red dots) and fit (blue curve) to the oscillatory signal corresponding to the 0.3 eV electron band (2, red in figures 1 and 2). The arrow indicates the onset at 200 fs of the damped 550 fs oscillating regime. The black dashed line indicates the cross correlation function of the pump/probe laser pulses (Gaussian FWMH=100 fs) which accounts for the time resolution of the present experiment in the fit.

Femtosecond pump probe experiments with 800 nm detection

The 800 nm probe always gives an excellent signal to noise ratio in pump/probe experiments as shown in figures 4 and 5, owing to the small background due to this probe even at high energies. However, when detecting photoelectrons, the higher number of probe photons makes the interpretation of the time resolved photoelectron spectra more complex through overlapping contribution of a different number of photons. Also the high ionization potential of benzophenone at 9 eV [25], requires in minimum 3 photons from S_2 and 4 from S_1 and T_1 (see figure 12). Thus the absolute detectivity with 800 nm probe is highest for the initial step, but the relative detectivity of S_1 and T_1 lower, as compared to that of 400 nm photons

The time decays obtained by the detection of these Gaussian components of the electron bands appears in figure 5 and shows similar features to the 400 nm detection: similar time components are found 150 fs /5 ps /400 ns plateau (decay determined later in ns experiments), with lower cross sections for the long time constants compared to the 400 nm probe. The ordering of the efficiency is similar as a function of electron energy. However, no risetime is detected in the kinetics and no oscillations can be observed. Another difference is the detection of weak higher order polarizations in the electron angular dependence (β_4) due to the greater number of photons in the ionization. Also the initial decay is similar here to the 400 nm detection. On the other hand, τ_2 was determined here more accurately due to the lower intensity of the final plateau (insert in figure 5) and the absence of oscillations in the decay.

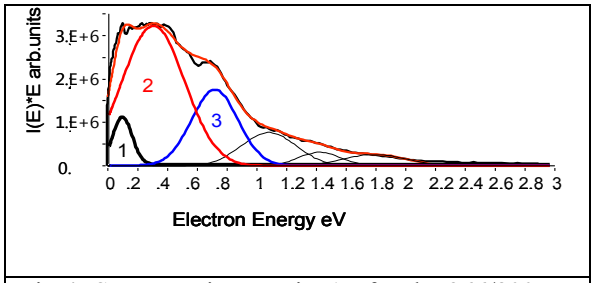

Fig 4: Same caption as Fig. 1, for the 266/800 nm pump/probe experiment.

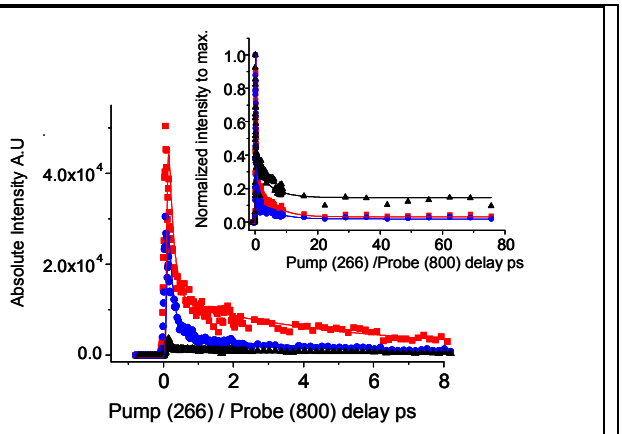

Fig 5: Time evolution of the photoelectron bands at 0.1, 0.3 and 0.7 eV selected in figure 4 and displayed with same colour code. Insert: maximum intensity normalized time evolution over 80 ps, showing the ns plateau.

At very long times (<80 ps), a ns plateau is detected for all electron energies and best seen at the lowest electron energies as appears in the insert of figure 5, in black, similarly to figure 1. The relative detection of the long lived time constant (ns) is not strikingly dependent upon the polarization component using, when analyzing the data with the pBASEX method and extracting the $\sigma(t)$ $\beta(t)$ components of the n^{th} order Legendre expansion.

Cluster deposited femtosecond experiments

The same experiments have been performed for benzophenone deposited on argon clusters, using a pick up technique [20], in order to observe the effect of a simple medium on the relaxation mechanisms. Both detections were used, but only the more efficient 800 nm detection gave results. The photoelectron spectrum is unpolarised and broad. It is analysed with nearly the same components except for the Gaussian component (1) at 0.15eV. All components are 10% broader, as appears in figure 6. The same general multiexponential behavior has been observed, similar to that of the free molecule but with striking variations. A triexponential model has been used and a fast 140 fs decay initiates the evolution, followed by a 20 ps decay onto the final evolution longer than μs, (figure 7). It is found that the photoelectron signal originates only from deposited benzophenone since for ion detection in time of flight measurements, no signal is detected at the free benzophenone mass, which further ensures the absence of contamination of the signal by free benzophenone. Benzophenone remains on the cluster, while the excess energy is disposed on the cluster.

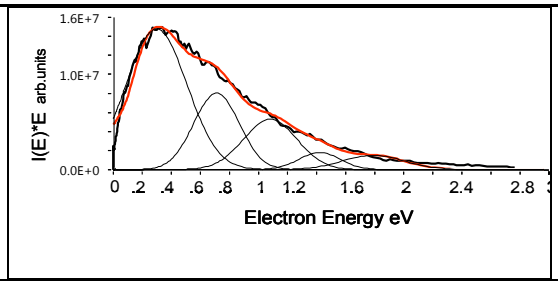

Fig 6: Isotropic component P_0 of the time integrated photoelectron spectrum (given as I(E)×E) in the 266/800 nm pump/probe experiment with benzophenone deposited on argon clusters (wiggly black curve). The red curve is a fit using Gaussian functions centred at 0.3, 0.7,… eV. Only the band at 0.3 eV (centre and width) is univocally determined from the spectrum. They have no specific physical content.

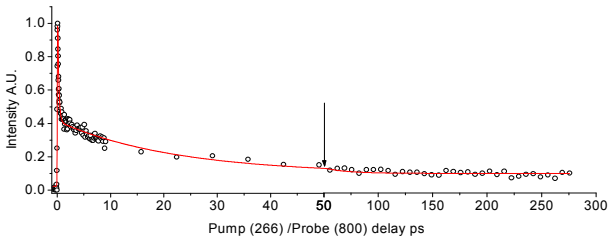

Fig 7: Time evolution of band 1 at 0.3 eV in figure 6 over 250 ps. Note the change in the horizontal linear scale at the arrow: [-.5,50 ps] below and [50,300 ps] after the arrow.

Nanosecond time evolution of free and deposited benzophenone

Nanosecond evolution has been observed in order to investigate the nature of the decay of the nanosecond long lived states in the case of free and deposited benzophenone. In 1+1' pump probe experiments, the photoelectron spectrum of the 'final states' can be recorded. With 266

pump+193 nm delayed probe, a rather diffuse photoelectron spectrum is observed decaying from E=0 eV (see figure 8) where the intensity I(E) is plotted directly with E without modification, in contrast with the previous figures. The signals of the sole pump and probe have been subtracted using an image taken at negative delays. It was verified that this negative time contribution was identical to the sum of the pump and probe independent contributions. The resulting photoelectron signal is shown in figure 8 and extends to 0.75 eV. It can be modeled by two Gaussian functions with energy close to 0 eV, for the free benzophenone. The maximum energy, 0.45 eV, by simple energy balance, corresponds to an electronic level at ~3 eV : E=ionization potential (9 eV) [25] –probe photon energy (6.42) + electron kinetic energy (0.45). There is a small contribution on the graph of another broad peak centered at 0.5 eV, which by its oven temperature dependence, can be linked to a benzophenone cluster, since it appears only at higher temperatures and large benzophenone concentrations.

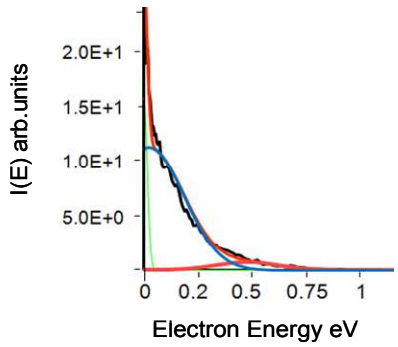

Fig 8: Photoelectron spectrum (given as I(E)) for free benzophenone, time integrated in the 266 / 193 nm nanosecond pump/probe experiment (black curve). The red curve passing through the experimental data is a fit using the the Gaussian functions given by the green, blue and red curves. The latter red curve depends upon benzophenone concentration and corresponds to the dimer.

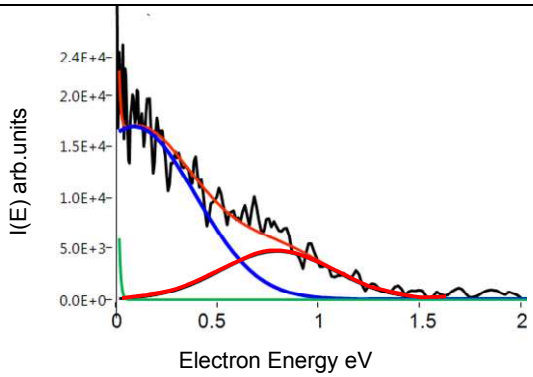

Fig 9: Same caption as Fig.8, when benzophenone is deposited on argon clusters. A 0.2 eV shift of the blue band in fig 8 is observed, together witha similar shift and a greater intensity of the 'dimer' band (red).

The same investigation is reported in figure 9 when benzophenone is deposited on argon clusters by the pick-up technique. A shift of these bands by +0.2 eV to higher energies was observed.

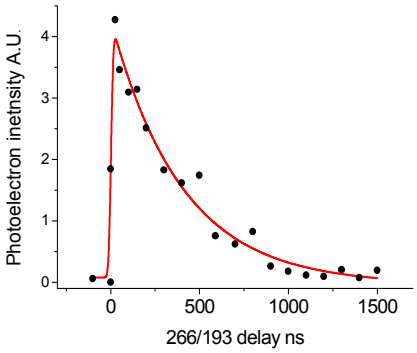

Fig 10: Time evolution of the free benzophenone photoelectron signal in the 266/193 nm nanosecond pump/probe experiment (black dots). The red curve is a fit with a single exponential, convoluted by the time resolution of the experiment), which reveals the final T_1-S_0 decay.

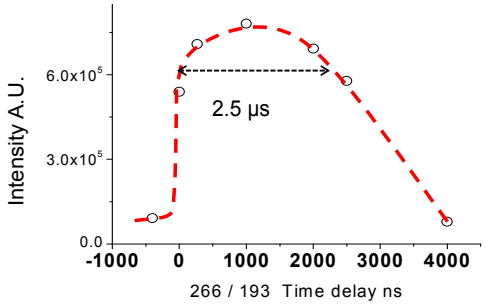

Fig 11: Same caption as Fig. 10, when benzophenone is deposited on argon clusters. The dotted red curve is simply for guiding the eye..

Monitoring the intensities of the major peak in the photoelectron spectrum allows tracing the time decay of the 'final ' states. This is the case, since the 193 nm detection probes T_1, the lowest electronic state of benzophenone. As is seen in figure 10, the decay can be fitted by a single exponential of 400±50 ns for the free molecule after excitation at 266 nm, while for benzophenone deposited on clusters, it is much longer than 2.5 µs, the limit of pump / probe observations. The evolution shown in figure 11 displays only a flat top time dependence as delineated by the arrow. This width of the maximum ~2.5 µs is determined by the overlap in time of the pump 1 mm and probe 5 mm beams as defined by the speed of the molecules 1800 m/s in an helium expansion, 2.7 µs.

Experiment	Femtosecond 266/400 nm	Femtosecond 266/800 nm	Femtosecond 266/400 nm and 266/800	Nanosecond 266/193 nm
Type of relaxation	S_2-S_1	S_2-S_1	S_1-T_1	T_1-S_0
Free benzophenone	150±30 fs Oscillations 550±10 fs	150±20 fs	5±0.5 ps	400±50 ns
Deposited benzophenone	-	140±20 fs	20±2 ps	>2μs

Table 1 : Time constants derived from the fit to the experiments results of figures 2, 3, 5, 7, 10 and 11. The types of relaxation to which the time constants are referred are determined in the discussion.

Discussion

Our experiments allow the observation of the complete relaxation dynamics of free and deposited benzophenone from the incipient electronic excitation to its final return to the ground state. The time evolution results are gathered in table 1: the rapid initial $\tau_{1=}$150 fs evolution is followed by a $\tau_{2=}$5 ps decay (20 ps when benzophenone is deposited) to a >300 ps plateau. Then a nanosecond detection reveals a slow decay in the μs range, in the complete absence of collisions. The latter evolution can be characterised as the return to the ground state.

Monitoring the evolution with photoelectron spectra

In time resolved pump-probe experiments, where a multiphoton probe generates photoelectron spectra of the evolving state initiated by the pump, these spectra carry essential informations on the identification of the evolving electronic state, through the energy of the photoelectrons and their polarisation with respect to the probe. Several effects smear out the information in the spectra.

When the probe operates in a quasi-resonant mode through high electronic states of the system, the shape of the individual bands in the photoelectron spectrum reflects the accessed relay state, and in turn the energy of the probed evolving state. It is also broadened through the absorption in each resonant short lived relay state.. In addition, autoionisation for the bands close to $E_{electrons}$=0 is generally very important and adds an unpolarized decaying quasi continuum to the structured

photoelectron spectra[26]. Another adverse effect obscures the interpretation when the resonant intermediate state reached by the probe decays during the probe pulse. In that case, the photoelectron spectra do not correspond to an image of the evolving state. Instead, it is a fingerprint of the higher lying states which serve as relay for the probe [27] with loss of information on the probed state.. In the multiphoton ionisation of phenols [27], these fingerprint states are typically a series of adjacent Rydberg states..

We have encountered here an intermediate situation, where each band in the transient photoelectron spectra cannot be assigned uniquely to a single electronic state S_2-S_1-T_1 of the evolving transient. Nevertheless, specific bands can be selected in the spectra that characterise uniquely each of S_2-S_1 or T_1 states. This is best observed with the 400 nm probe as in figure 2, where the 3 bands exhibit a different behavior. Band 2 favors the observation of S_2, while band 1 favors the final state and band 3 shows the least preference.

i) The position of band 1 at E=.1 eV is understood easily from the ionisation energetics of T_1 with: $E=(E_{tripletT1},3.eV)+2*(E_{397nm},6.2eV)=9.2$ eV, matching the ionisation potential of benzophenone, which is ~9eV[25]. ii) In turn, band 3 with maximum at 0.7 eV, favouring S_2 through its highest initial intensity, is found below the resonant ionisation of S_2. Its maximum extension comes to 1.1 eV, compared to the threshold at 1.5 eV [13]. This shift can be due to Franck-Condon excitation of high vibrational levels of the intermediate level as depicted in figure 12 through S_n and this vibrational excitation is transposed into the ion levels causing the shift. iii) Band 3 broad and centered at 0.3 eV, shows the least preference for S_2, S_1 or T_1. This could result from the relaxation of the intermediate reached by the probe after excitation of S_2.

The observation of bands 3 (preference for S_2) and 1 (preference for S_1,T) allows a good identification of the decays of respectively S_2 and S_1,T.

Monitoring Triplet formation and decay

In the condensed phase, the formation of the triplet benzophenone has been well established by triplet-triplet absorption and proceeds with a time constant of 16 ps in ethanol at 355 nm[5] and 10 ps at 267 nm and 383 nm[28]. It has a quasi-unit efficiency of formation [29]. Thus after 10ps, the benzophenone in the liquid phase is essentially in the triplet state.

In the gas phase, the electronic species that we detect in the nanosecond range shows a threshold electronic energy of ~2.94eV or lower from its transient nanosecond photoelectron spectrum. This accords with the vibrationless $T_1(n,\pi^*)$ state at 3eV [30]. The resultant state from electronic relaxation, after excitation at 266 nm, has a high vibrational energy content of 1.66 eV. Likely, in the ns time range, this excitation has been randomised by vibrational redistribution over the available 66 vibrational degrees of freedom. In the $T_1(n,\pi^*)$ excited state, one electron from the oxygen lone pair has migrated over the benzene rings causing a decrease in the angle of the benzene rings with the >C=O plane [3] and generating vibrational excitation along this coordinate. The one photon ionization should be direct from the lowest triplet T_1 (n,π^*) through the departure of the π^* electron and the formation of the ground state ion (n-1) on the oxygen atom. Aside from progressions on the C-phenyl torsional mode, the threshold electron energy can reflect the electronic level position of the T_1 electronic state. We hence assign the threshold photoelectron energy with the ionisation of the lowest $T_1(n,\pi^*)$ state. Thus by extension, the plateau observed at times 10 ps -1 ns characterises the detected state as T_1, in correspondance with condensed phase experiments. We shall discuss later the variations in lifetimes of T_1 between the various phases.

Ultrafast measurements: from the initial state S_2 to the lowest triplet T_1

Step1 -decay of the S_2 state,

The initial decay of the S_2 state is readily observed for the 800 nm probe and appears also with 400 nm detection. There, the initial decay at electron energies >0.3eV is matched by the growth of a signal at 0 <E< 0.3eV with the same 150 fs time constant. This short time constant is characteristic of a rapid wavepacket evolution through a surface crossing via a conical intersection and the strong decrease in the photoelectron intensity from the product state indicates a state much lower in energy than S_2. Transient absorption measurements in acetonitrile solutions have shown the characteristic appearance of the S_1-S_n absorption after 530 fs [17]. The reduction in lifetime in the gas phase can be ascribed to the absence of the viscosity of the solvent slowing down the initial wavepacket. The evolution from the initially excited state leads to a hot S_1 state in isolated conditions. This S_2-S_1 evolution is quite interesting here because its appearance is devoid of a typical ultrashort component revealing a rapid spread of the initial wavepacket over the excited potential energy surface (PES). Very often indeed, steep slopes about the Franck Condon zone on the excited PES spread the wavepacket and drive it to the conical intersection.

As discussed below, the S_2-S_1conical intersection in benzophenone is apparently close to the Franck Condon region and is reached before a substantial spread of the wavepacket.

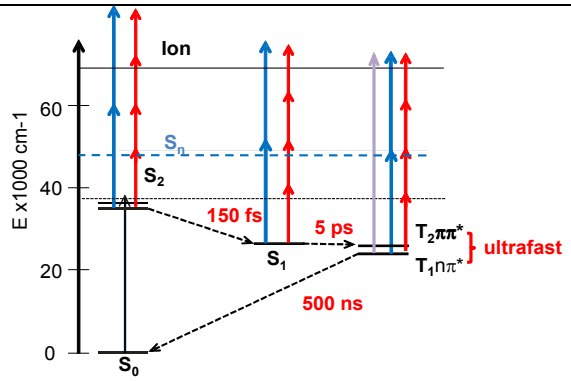

Figure 12: Schematics of the energetics of the evolution in benzophenone.

Step2: Wavepacket Oscillations in the S_1 state and decay,

This S_2-S_1 wavepacket evolution is accompanied by 550 fs oscillations (see figure 3), which correspond to a 61 cm^{-1} level separation. This value is close to the lowest frequency, 60 cm^{-1} assigned to the totally symmetric ring torsional frequency in the S_1 state [10, 11]. As noted earlier, the environment of the CO bond is differently affected by the electronic excitation, the most apparent in our experiments being the torsion angle of the benzene rings with respect to the >C=O plane due to its small force constant. Thus, the wavepacket created along the torsional coordinate shows oscillations in its ionization efficiency as a function of its position. This effect is likely enhanced in the 400 nm ionisation by the configuration of the resonance level.

The first maximum of the oscillations appears with a delay of ~300 fs with respect to the zero of time (autocorrelation). The resulting induction time for the oscillations in our simulations (200 fs) is close to the S_2-S_1 decay and the phenyl symmetric torsion mode is likely the crossing coordinate in the conical intersection. We can hypothesize that the descent of the wavepacket along this coordinate has created the excitation in same fashion as for the late creation of oscillations in TDMAE [31] and recently in pyrazine[32]. These oscillations disappear with the population of the S_1 state, after 4 oscillations, faster than could be expected from the anharmonicity.

The strong oscillations are superimposed on the decay of the S_1 state, occurring with a time constant of 5 ps for the free benzophenone molecule. In solutions, the appearance time of T_1 is 10 ps at 300 K [33, 28]. The gas phase 5ps decay time corresponds to the intersystem crossing from S_1, since we have identified the long lived state as T_1 and that no kinetics are apparent in the [>5ps, <100ns] time domain. Although a great variation of time constants has not been reported for the S_1-T_1 ISC lifetime[28], an energy gap law applies for this rate[34]. The argon deposited benzophenone has a small internal excess energy at 32 K after relaxation of the excess energy to the argon cluster as compared with the isolated gas phase benzophenone excited at 266 nm, ~14000 cm^{-1}. Therefore, the increase in ISC rate from the deposited molecule, to the liquid phase and to the gas phase is modest (x4) and has to be related with a quasi-direct process. In such case after a threshold is reached, no rate increase is observed [34].

S_1-T_1 Intersystem crossing

The quasi unit efficiency of the intersystem crossing in benzophenone has been the subject to ample questioning regarding the efficiency of the electronic coupling between S_1 and T_1. Reasoning in a planar geometry for benzophenone, the forbidden S_0 - S_1 transition leads to a $S_1(n\pi^*)$ state, which has a low spin orbit coupling with the $T_1(n\pi^*)$ state. Strong coupling results from a quasi resonant $T_2(\pi\pi^*)$ state with $S_1(n\pi^*)$ [30, 35]. Such a T_2 $(\pi\pi^*)$ state has been calculated[13] and is degenerate with S_1. However the delocalisation of the π^* orbital over the benzophenone molecule is only possible in the planar case, from which the benzophenone molecule deviates by a ~30° torsion for each benzene cycle. This certainly mixes the triplet $n\pi^*$ and $\pi\pi^*$ configurations and should allow a strong SO mixing, even in absence of an available resonant $T(\pi\pi^*)$ triplet state with $S_1(n\pi^*)$ [36].

In the case of isolated benzophenone excited at 266 nm, the first step in the evolution has been characterised in the isolated phase as the S_2-S_1 internal conversion, which creates a vibrationally hot S_1 state with ~1.4 eV of vibrational energy. Thus energetically, the system is above several $T_{n>1}$ states[13] and will find the desired coupling. The ensuing internal conversion in the triplet manifold is expected to be very fast, and should be similar to the S_2-S_1 IC (150 fs) and faster than the S_1-T decay time constant (5 ps). Thus this T_n-T_1 IC remains unnoticed in the time evolution and the evolution from the hot S_1 will appear as it proceeded directly to T_1. We indeed see no apparent change of the photoelectron spectrum through the lifetime of the S_1 state.

Step 3: Decay route of T_1

We have observed the decay of the lowest T_1 state of the isolated benzophenone in 400 ns, step 3 in the evolution. This value is in fair agreement with double resonance experiments by Zalesskaya et al. [37] pumping triplet levels with an infrared CO_2 laser, who find a 4.10^6 s^{-1} triplet decay rate (250 ns) for a 14000 cm^{-1} excess energy equivalent to the excess energy after 266 nm pumping. On the other hand, the very low decay rate on deposited benzophenone is consistent also with the long triplet lifetimes (ms) at 77 K.

The rapid decay of T_1 in the isolated molecule is associated with a loss of electronic excitation through the disappearance of the photoelectron spectrum in 266/193 nm experiments. This could be due to the α cleavage of ϕ-CO-ϕ in ϕ-CO+ ϕ. From reported thermochemistry, the threshold for this dissociation is close to 90 kcal= 3.9 eV, while Obi *et al.*[38] observed that from T_n as high as 5.73 eV, internal conversion to T_1 is the major decay path. Thus, we assign the decay of the T_1 state by intersystem crossing to the ground state S_0. This decay is mostly radiative, 5.2 ms at thermalized low temperatures[12], as in the case of the deposited benzophenone on argon. With a few hundreds of wavenumbers of excess energy at room temperature the decay becomes non radiative with a 3 μs lifetime [38] and follows the usual energy gap law at higher temperatures driven the dissipative Fermi golden law mechanism between T_1 and the quasi continuum of S_0.

Summary and Conclusion

We have revisited the triplet formation in gaseous benzophenone, excited in S_2, in complete isolation conditions, using time resolved photoelectron spectroscopy, from the very early moments of the evolution, to the return to the ground state. The decay is sequential with three major steps. In the first one, a rapid, 150 fs internal conversion populates the first excited singlet state. This wavepacket movement traversing the S_2-S_1 intersection is accompanied by intense oscillations that have a first maximum after the crossing. Their frequency matches the symmetric

mode of oscillation of the phenyls, one of the modes that are changed in the electronic excitation, with the observed 61 cm^{-1} level spacing deduced from the oscillation frequency.

The next step is the passage from S_1 to the triplet manifold in 5 ps, in isolated conditions. This value, only twice as short as the room temperature solution value, is high for a light organic molecule but is in accordance with the known but surprisingly efficient SO coupling for this molecule. Following El Sayed's rules[35] to obtain an efficient ISC requires a mediating T_2 ($\pi\pi^*$) state between S_1 ($n\pi^*$) and T_1 ($n\pi^*$). This state may exist but its evolution cannot be observed with the present experimental technique, since it is masked by the long 5ps lifetime. In similar experiments on pyrazine [23], where the couplings are equivalent, no intermediate T_2 ($\pi\pi^*$) could be evidenced either. The present work cannot distinguish between the passage in two steps S_1 ($n\pi^*$) $\rightarrow T_2$ ($\pi\pi^*$) $\rightarrow T_1$ ($n\pi^*$) or a single step towards a T_1 state with partial $\pi\pi^*$ character, as proposed in ref [36]. We nevertheless favour this view of a strongly mixed surface, since such a surface of mixed $\pi\pi^*$ and $n\pi^*$ character, angle dependent, has been recently characterised for 2-hydroxypyridine. There, one vibrational coordinate strongly couples both surfaces, i.e. an out of plane vibration[39]. Here the phenyl torsion might be the coupling coordinate, this being supported by the observed change in ionization cross sections along this coordinate. Therefore the T_2 'state' directly accessed may be simply considered as a region with a main $\pi\pi^*$ character rapidly traversed during the temporal evolution.

We could also model the medium effect on intersystem crossing from S_1 by depositing the benzophenone molecule on argon clusters. This is very interesting because it allows a perfect comparison between condensed and gas phase evolution with the same experimental methods. For deposited benzophenone, the excess energy from S_2 is rapidly evacuated on the cluster, while benzophenone remains attached to it, thus the effective temperature of the molecule drops to ~32 K. This slows down the rate of ISC by a factor of 4. The model developed by Engelman and Jortner [40] on the multilevel interaction and a strong coupling (with surface crossing) seems adapted to reproduce the behavior of the decay: below the barrier a slow decay excess energy dependent, above the barrier, little excess energy dependence above room temperature. The cluster further relaxes the triplet benzophenone molecule after ISC and no further decay of the triplet molecules can be observed in our conditions limited to a 2 μs time window. On the other

hand, for the free benzophenone molecule with high excess energy the intersystem crossing to S_0 could be monitored.

In summary, the T_1 state of benzophenone is produced by irradiation in S_2 in a quasi-statistical manner through S_1, in isolated conditions, by a sequential mechanism comparable to that observed for acetophenone, with a similar level structure[41]. There is no specific enhancement of the ISC efficiency from S_2 and the triplet is available for 400 ns for reactive encounters with a high excess energy. The sequential mechanism is the same in the gas and the 'deposited' cluster phase.

Acknowledgements

G.S. thanks EU-ITN project ICONIC-238671 for funding. L.P. thanks the ANR for support through the contract ANR-09-JCJC- 0090-01 CHROMADYNE. Furthermore, we thank the CEA/SLIC staff, in particular Olivier Gobert and Michel Perdrix, for technical support.

References

1. N. J. Turro, *Modern Molecular Photochemistry*, University Science Books Sausalito CA 94965, 1991.
2. G. N. Lewis and M. Kasha, *J. Am. Chem. Soc.*, 1944, 66, 2100.
3. R. Hoffmann and J. R. Swenson, *J. Phys. Chem.*, 1970, 74, 415.
4. B. Mordechai and J. Joshua, *J. Chem. Phys.*, 1968, 48, 715.
5. R. S. Minns, D. S. N. Parker, T. J. Penfold, G. A. Worth and H. H. Fielding, *Phys. Chem. Chem. Phys.*, 2010, 12, 15607.
6. T. J. Penfold, R. Spesyvtsev, O. M. Kirkby, R. S. Minns, D. S. N. Parker, H. H. Fielding and G. A. Worth, *J.Chem.Phys.*, 2012, 137, 204310.
7. M. H. Ha-Thi, N. Shafizadeh, L. Poisson and B. Soep, *J. Phys. Chem. A*, 2013, 117, 8111.
8. R. M. Hochstrasser, H. Lutz and G. W. Scott, *Chem. Phys. Lett.*, 1974, 24, 162.
9. S. Aloise, C. Ruckebusch, L. Blanchet, J. Rehault, G. Buntinx and J.-P. Huvenne, *J. Phys. Chem. A.*, 2007, 112, 224.
10. K. W. Holtzclaw and D. W. Pratt, *J. Chem. Phys.*, 1986, 84, 4713.
11. S. Kamei, T. Sato, N. Mikami and M. Ito, *J.Phys.Chem*, 1986, 90, 5615.
12. S. Dym and R. M. Hochstrasser, *J. Chem. Phys.*, 1969, 51, 2458.
13. T. V. Bezrodnaya, V. I. Mel'nik, G. A. Puchkovskaya and L. I. Savranskii, *Journal of Structural Chemistry*, 2006, 47, 194.
14. M. A. El-Sayed, *J.Chem.Phys.*, 1963, 38, 2834.
15. T. Bezrodnaya, V. Mel'nik and K. Nelipovich, *J. Mol. Struct.*, 2001, 596, 55.
16. G. E. Busch, P. M. Rentzepis and J. Jortner, *J.Chem.Phys.*, 1972, 56, 361.
17. B. K. Shah, M. A. J. Rodgers and D. C. Neckers, *J. Phys. Chem. A.*, 2004, 108, 6087.

18. J. Köhler, P. Hemberger, I. Fischer, G. Piani and L. Poisson, *J. Phys. Chem. A.*, 2011, 115, 14249.
19. E. Gloaguen, J. M. Mestdagh, L. Poisson, F. Lepetit, J. P. Visticot, B. Soep, M. Coroiu, A. Eppink and D. H. Parker, *J. Am. Chem. Soc.*, 2005, 127, 16529.
20. S. Awali, L. Poisson, B. Soep, M.-A. Gaveau, M. Briant, C. Pothier, J.-M. Mestdagh, M. B. E. H. Rhouma, M. Hochlaf, V. Mazet and S. Faisan, *Phys. Chem. Chem. Phys.*, 2014, 16, 516.
21. S. Soorkia, C. Pothier, M. Mestdagh, B. Soep and J. Lievin, *J. Phys. Chem. A*, 2010, 114, 5655.
22. G. A. Garcia, L. Nahon and I. Powis, *Rev. Sci. Instrum.*, 2004, 75, 4989.
23. J. K. Song, M. Tsubouchi and T. Suzuki, *J. Chem. Phys.*, 2001, 115, 8810.
24. J. Cooper and R. N. Zare, *J.Chem.Phys.*, 1968, 48, 942.
25. G. Centineo, I. Fragala, G. Bruno and S. Spampinato, *J. Mol. Struct.*, 1978, 44, 203.
26. E. Gloaguen, J. M. Mestdagh, L. Poisson, F. Lepetit, J. P. Visticot, B. Soep, M. Coroiu, A. T. J. B. Eppink and D. H. Parker, *J. Am. Chem. Soc.*, 2005, 127, 16529.
27. J. L. Gosselin and P. M. Weber, *J. Phys. Chem. A*, 2005, 109, 4899.
28. S. Aloise, C. Ruckebusch, L. Blanchet, J. Rehault, G. Buntinx and J.-P. Huvenne, *J. Phys. Chem. A.*, 2007, 112, 224.
29. M. Terazima and N. Hirota, *J.Chem.Phys.*, 1991, 95, 6490.
30. S. P. McGlynn, Azumi T. and K. M., *Molecular Spectroscopy of the Triplet State*, Prentice - Hall, New Jersey, 1969
31. S. Sorgues, J. M. Mestdagh, J. P. Visticot and B. Soep, *Phys. Rev. Lett.*, 2003, 91, 1.
32. T. Suzuki, *International Reviews in Physical Chemistry*, 2012, 31, 265.
33. R. W. Anderson Jr, R. M. Hochstrasser, H. Lutz and G. W. Scott, *Chem. Phys. Lett.*, 1974, 28, 153.
34. R. Englman and J. Jortner, *Molecular Physics. Jan.*, 1970, 18, 145.
35. M. A. El-Sayed, *Acc. Chem. Res.*, 1968, 1, 8.
36. G. Wackerle, M. Bar, H. Zimmermann, K. P. Dinse, S. Yamauchi, R. J. Kashmar and D. W. Pratt, *J. Chem. Phys.*, 1982, 76, 2275.
37. G. A. Zalesskaya, D. L. Yakovlev, E. G. Sambor and N. N. Bely, *Phys. Chem. Chem. Phys.*, 2002, 4, 5634.
38. Y. Takatori, T. Suzuki, Y. Kajii, K. Shibuya and K. Obi, *Chem. Phys.*, 1993, 169, 291.
39. L. Poisson, D. Nandi, B. Soep, M. Hochlaf, M. Boggio-Pasqua and J.-M. Mestdagh, *Phys. Chem. Chem. Phys.*, 2014, 16, 581.
40. R. Englman and J. Jortner, *Mol. Phys.*, 1970, 18, 145.
41. S. T. Park, J. S. Feenstra and A. H. Zewail, *J. Chem. Phys.*, 2006, 124.